Room temperature hyperpolarization of nuclear spins in bulk

Kenichiro Tateishi[a,b,1], Makoto Negoro[a,1,2], Shinsuke Nishida[c,3], Akinori Kagawa[a], Yasushi Morita[c,3], and Masahiro Kitagawa[a]

[a]Department of Systems Innovation, Division of Advanced Electronics and Optical Science, Graduate School of Engineering Science, Osaka University, Toyonaka, Osaka 560-8531, Japan; [b]RIKEN Nishina Center for Accelerator-Based Science, Wako, Saitama 351-0198, Japan; and [c]Department of Chemistry, Graduate School of Science, Osaka University, Toyonaka, Osaka 560-0043, Japan

Edited by Jack H. Freed, Cornell University, Ithaca, NY, and accepted by the Editorial Board April 16, 2014 (received for review August 20, 2013)

Dynamic nuclear polarization (DNP), a means of transferring spin polarization from electrons to nuclei, can enhance the nuclear spin polarization (hence the NMR sensitivity) in bulk materials at most 660 times for ^{1}H spins, using electron spins in thermal equilibrium as polarizing agents. By using electron spins in photo-excited triplet states instead, DNP can overcome the above limit. We demonstrate a ^{1}H spin polarization of 34%, which gives an enhancement factor of 250,000 in 0.40 T, while maintaining a bulk sample (~0.6 mg, ~0.7 × 0.7 × 1 mm^3) containing >10^{19} ^{1}H spins at room temperature. Room temperature hyperpolarization achieved with DNP using photo-excited triplet electrons has potentials to be applied to a wide range of fields, including NMR spectroscopy and MRI as well as fundamental physics.

sensitivity enhancement | regioselective deuteration | pentacene | quantum simulation | polarized target

Nuclear spin is a useful probe for noninvasive analysis of bulk materials such as chemical compounds, industrial products, biological samples, and human bodies. The signal from a spin ensemble is proportional to the polarization P. In thermal equilibrium in a magnetic field B at temperature T, P for spin-1/2 particles is given by

$$P = \tanh\left(\frac{\hbar\gamma B}{2kT}\right), \quad [1]$$

where $\hbar$ is the Planck constant, k is the Boltzmann constant, and γ is the gyromagnetic ratio. In a magnetic field of several teslas at room temperature, the nuclear spin energy $\hbar\gamma B/2$ is much smaller than the thermal energy kT, so nuclear spins are only slightly polarized. This is the major reason why the sensitivity of NMR spectroscopy and MRI is so low.

Dynamic nuclear polarization (DNP) is a means of transferring spin polarization from electrons to nuclei. As a method to enhance the bulk nuclear polarization, DNP has been successfully applied to areas ranging from fundamental physics (1–3) to materials science (4), biology (5–7), and medical science (8), since it was discovered 60 y ago (9, 10). As long as electron spins in thermal equilibrium are used as polarizing agents, the upper limit of the polarization enhancement is 660 for ^{1}H spins and cryogenic temperatures of around 4.2 K are required for hyperpolarization in the order of 10% even in the strong magnetic fields used for NMR. Hyperpolarization at room temperature will simplify instrumentation and expand the sample variety to materials that prefer ambient temperatures. Other techniques such as optical pumping in semiconductors (11) and the Haupt effect (12) also require cryogenic temperature for increasing bulk polarization beyond 10%.

One solution for overcoming the upper limit of the enhancement factor of the conventional DNP, γ_e/γ_n, is to use nonthermalized electron spins as polarizing agents. A number of organic molecules have photo-excited triplet states where, due to the selection rule in the intersystem crossing from the excited singlet state to the triplet state, the population distribution is highly biased. DNP using electron spins in the photo-excited triplet state can achieve hyperpolarization independent of the magnetic field strength and temperature (13–16). In this work, we have achieved a bulk hyperpolarization of 34% and corresponding to 250,000 times enhancement in 0.40 T at room temperature with the following procedure.

The procedure, developed by Henstra et al. (13), begins with shining a pulsed laser to excite the polarizing agents, e.g., a pentacene dopant in the sample. The energy diagram is shown in Fig. 1*A*. The hyperpolarization in the photo-excited triplet state is transferred to nuclear spins in the vicinity during the triplet lifetime by a pulsed DNP process, the integrated solid effect (ISE) (13). In the process, the field sweep and microwave irradiation near the transition frequency between the triplet sublevels are simultaneously applied, as shown in Fig. 1*B*. The inhomogeneously broadened electron spin packets are adiabatically swept over, and the effective nutation frequency of the electron spins in the rotating frame is matched with the ^{1}H spin Larmor frequency at some point of the adiabatic process. The photo-excited triplet state decays nonradiatively to the ground singlet state. The hyperpolarized spin state diffuses from the nuclear spins in the vicinity of the polarizing agent to the whole sample. This sequence can be repeated to accumulate nuclear spin polarization until the buildup and the nuclear spin-lattice relaxation reach steady state. In ref. 13, at room temperature in 0.35 T, the polarization of ^{1}H spins was increased to 0.66%,

Significance

Nuclear spins are only slightly aligned even in the strong magnetic fields of superconducting magnets because the magnetic energy of nuclear spin is much smaller than thermal energy. This is the major reason for the low sensitivity of NMR spectroscopy. Using electron spins in thermal equilibrium, which have 660 times higher magnetic energy, the sensitivity can be enhanced by at most this factor through a method called dynamic nuclear polarization. Utilizing photo-excited nonthermalized electrons instead, we demonstrate an enhancement factor of 250,000 at room temperature, which can be applied to a wide range of fields including NMR, MRI, and physics.

Author contributions: K.T., M.N., Y.M., and M.K. designed research; K.T. and M.N. performed research; K.T., S.N., A.K., and Y.M. contributed new reagents/analytic tools; K.T. and M.N. analyzed data; and K.T., M.N., and M.K. wrote the paper.

The authors declare no conflict of interest.

This article is a PNAS Direct Submission. J.H.F. is a guest editor invited by the Editorial Board.

[1]K.T. and M.N. contributed equally to this work.

[2]To whom correspondence should be addressed. E-mail: negoro@ee.es.osaka-u.ac.jp.

[3]Present address: Department of Applied Chemistry, Faculty of Engineering, Aichi Institute of Technology, Toyota 470-0392, Japan.

This article contains supporting information online at www.pnas.org/lookup/suppl/doi:10.1073/pnas.1315778111/-/DCSupplemental.

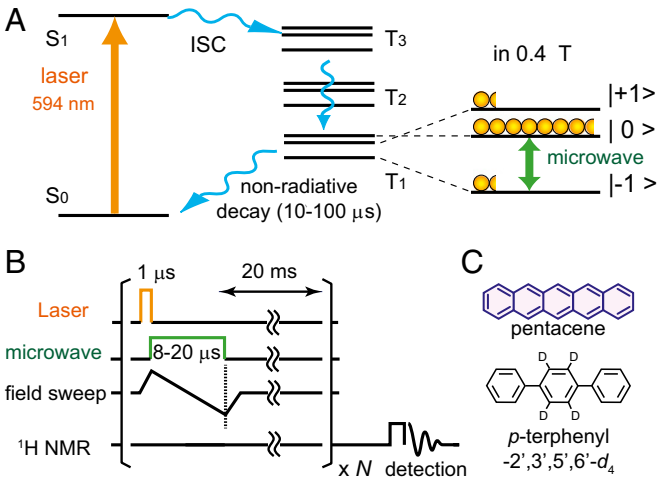

Fig. 1. Pentacene doped in a *p*-terphenyl crystal and pulse sequence for DNP. (*A*) Energy diagram of pentacene doped in a *p*-terphenyl crystal. An electron excited with laser irradiation transits to a triplet state by intersystem crossing (ISC) and decays to the lowest triplet state. In a magnetic field of 0.40 T applied in parallel along the long molecular axis of pentacene, the energy gap between $|0\rangle$ and $|-1\rangle$ is ~12 GHz, and the populations of the triplet sublevels are 12%, 76%, and 12%, respectively (17). The triplet state decays in 10–100 μs (18). (*B*) Pulse sequence for DNP and NMR detection. (*C*) Pentacene and *p*-terphenyl-2′,3′,5′,6′-d_4.

which gave an enhancement factor of 5,500 in a single crystal of naphthalene doped with 0.01 mol% pentacene.

We adopted *p*-terphenyl as a host material instead of naphthalene, because it does not sublimate at room temperature. To the best of our knowledge, until now the highest enhancement factor at room temperature was 13,000 in 0.3 T with a ^{1}H spin polarization of 1.3%. This was achieved with a *p*-terphenyl host material (19). We did the DNP experiments in 0.40 T at room temperature. In Fig. 2 T*h*P*h* shows the buildup curve of ^{1}H spin polarization in a single crystal of *p*-terphenyl-h_{14} doped with pentacene-h_{14}, 0.05 mol%. By carefully optimizing the ISE parameters and avoiding sample heating, we attained a ^{1}H spin polarization of 14% (see *SI Text* for experimental details, the polarization transfer mechanism, and the method to determine the polarization).

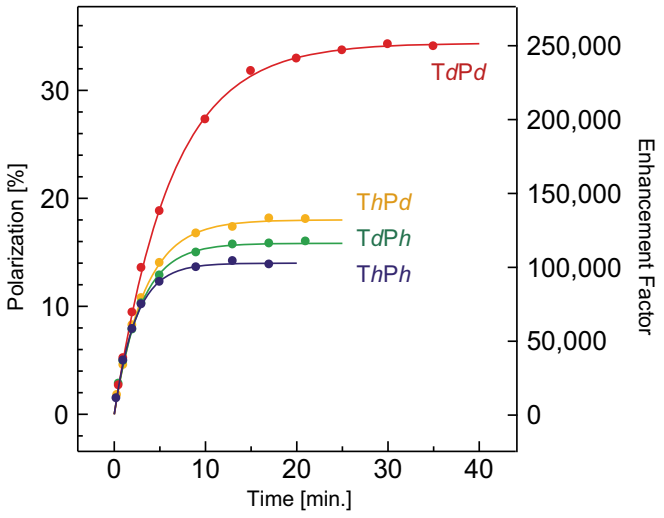

Fig. 2. Polarization buildup curves. Blue, green, yellow, and red indicate the polarization buildup curves using T*h*P*h*, T*d*P*h*, T*h*P*d*, and T*d*P*d*, respectively. T*h*, T*d*, P*h*, and P*d* mean *p*-terphenyl-h_{14}, *p*-terphenyl-2′,3′,5′,6′-d_4, pentacene-h_{14}, and pentacene-d_{14}, respectively. The polarizations and enhancement factors were estimated by comparing the intensities of the hyperpolarized signals and the thermal signal in 0.40 T at room temperature.

The key breakthrough in the present work to attain higher polarization at room temperature is partial deuteration of the sample. Our purpose is suppression of spin-lattice relaxation, whereas the technique blending fully deuterated molecules in the host matrix often used in conventional DNP is for decreasing the number of spins in the host matrix when spins of interest are sparsely distributed in the sample (6). In practice, the attainable ^{1}H polarization is limited by the ^{1}H spin-lattice relaxation time. The spin-lattice relaxation time of the ^{1}H spins in the *p*-terphenyl-h_{14} host crystal, T_{1n}, was 11 min at room temperature. The ^{1}H spin-lattice relaxation was mainly due to the pendulum motion of the central benzene ring, which modulates the local dipolar field of the ^{1}H spins in and near the central ring (20). To suppress the spin-lattice relaxation, we synthesized regioselectively deuterated *p*-terphenyl-2′,3′,5′,6′-d_4 (Fig. 1*C*) (see *SI Text* for details of organic synthesis). T_{1n} of the regioselectively deuterated sample with the deuteration ratio 4/14 = 28.6% is four times longer than the nondeuterated sample, whereas T_{1n} of the sample blending 30% fully deuterated *p*-terphenyl-*d*14 and 70% nondeuterated *p*-terphenyl-*h*14 remains almost the same as the nondeuterated sample (21). Therefore, T_{1n} was increased owing to the regioselective deuteration. The attainable polarization $P_{\rm fin}$ was increased to 16% in the regioselectively deuterated host doped with pentacene-h_{14} (T*d*P*h* in Fig. 2). However, the improvement was disappointing.

There is another source of ^{1}H spin-lattice relaxation that affects DNP. We noticed that the triplet electrons play the role of polarizing agent as well as contribute to spin-lattice relaxation of the ^{1}H spins in the vicinities through a perturbation of the local field of the ^{1}H spins. In the case of photo-excited triplet electrons, the effect of the spin-lattice relaxation of the vicinities is propagated to the whole sample because of the absence of the so-called spin diffusion barrier. The ^{1}H spin-lattice relaxation time attributed to the triplet electrons, defined as T_{1e}, can be estimated using $1/T_{1e} = 1/T_{1\rm laser} - 1/T_{1n}$, where $T_{1\rm laser}$ is the measured ^{1}H spin-lattice relaxation time under the pulsed laser irradiation without microwave irradiation (Table 1). By deuteration of the pentacene, T_{1e} can be increased by a factor of *ca.* 1.6. The deuteration of triplet molecules was already reported (22, 23). However, the purpose was to clarify the polarization transfer mechanism in refs. 22–24. Although the interactions between the triplet electrons and the surrounding ^{1}H spins are weakened in the sample with the deuterated pentacene, a polarization transfer efficiency comparable to that in a sample with pentacene-h_{14} can be obtained for a longer ISE duration, as also reported in ref. 23. In fact, by using *p*-terphenyl-h_{14} doped with pentacene-d_{14} (T*h*P*d* in Fig. 2), the initial gradient of the buildup curve, $dP(t)/dt|_{t=0}$, was almost the same as T*h*P*h*, as shown in Table 1.

Table 1. ^{1}H spin-lattice relaxation times and the fitting parameters of the buildup curves

Sample*	$T_{1n}^{\dagger}$	$T_{1\rm laser}$	T_{1e}	$\left.\frac{dP(t)}{dt}\right\|_{t=0}$	$P_{\rm fin}$	τ
Unit	min	min	min	%/min	%	min
T*h*P*h*	11	6.0	13.2	5.8	14	2.4
T*d*P*h*	37	10.6	14.9	5.5	16	2.9
T*h*P*d*	11	7.3	21.7	5.5	18	3.3
T*d*P*d*	37	18.9	38.6	5.5	34	6.2

*The denotation is the same as in Fig. 2.

†The relaxation times $T_{1\rm laser}$ and T_{1n} were measured with and without the pulsed laser irradiation at the repetition rate of 50 Hz, respectively. T_{1e} is the electron contribution in $T_{1\rm laser}$. The initial gradient $dP(t)/dt|_{t=0}$ of the polarization buildup curve, fitted by $P(t) = P_{\rm fin}(1 - e^{-t/\tau})$, was calculated by $P_{\rm fin}/\tau$.

The attainable polarization P_{fin} was increased to 18%. Again the improvement was disappointing.

Suppressing either of the two relaxation sources was not enough. What if a method of suppressing both of them was established? By using *p*-terphenyl-2′,3′,5′,6′-d_4 doped with pentacene-d_{14} (T*d*P*d* in Fig. 2), we achieved a bulk ^{1}H spin polarization of 34% at room temperature in 0.40 T, which gives an enhancement factor of 250,000, much larger than 13,000 that was previously reported for DNP using electron spins in photo-excited triplet states at room temperature (19) and far larger than 660, the upper limit of the conventional DNP using electron spins in thermal equilibrium. The achieved transfer efficiency, ~47%, of electron spin polarization to nuclear spins was non-trivial because the theoretical limit of the efficiency of the Overhauser effect is 50% and the efficiencies in most biological studies using solid effect and thermal mixing are less than 50%. The achieved ^{1}H spin polarization of 34% means that two-thirds of the $>10^{19}$ ^{1}H spins contained in the bulk sample can be aligned in the same direction. The ^{13}C cross-polarization (CP) spectrum of the hyperpolarized sample, shown in Fig. 3, provides further evidence of such a high polarization. The spectrum is split by the dipolar interaction with the nearest-neighbor ^{1}H spin and each peak height represents the population of the ^{1}H spin state. Sufficiently long DNP makes the asymmetrical character of the doublet spectrum very clear. The polarization determined from the asymmetry is 34% (1, 25, 26), which agrees with the polarization calculated from the comparison of the intensities of the hyperpolarized and thermal signals (details in *SI Text*).

Room temperature hyperpolarization techniques using photo-excited triplet electrons simplify DNP experiments and have the potential to be applied to a wide range of fields. The polarization of 34% is 8,500 times higher than the thermal polarization of ^{1}H spins in 11.7 T at room temperature. NMR sensitivity of samples that prefer ambient temperatures can be boosted significantly. Using photo-excited triplet electrons can increase the DNP enhancement factor in a method proposed for hyperpolarizing flow liquids (27). To achieve the polarization of 34% in conventional DNP at 11.7 T, the temperature should be much lower than the liquid nitrogen temperature. The conventional DNP at cryogenic temperature needs special equipment to make it compatible with the standard high-resolution NMR spectroscopy or MRI (4–8). Using photo-excited triplet electrons, this can be simplified. The ^{13}C CP spectrum in Fig. 3 was obtained in a homogeneous superconducting magnet of 11.7 T with our field cycling instrumentation (28), which is similar to that in ref. 5. For the applications to high-resolution NMR spectroscopy and MRI, we need additional equipment for dissolving, magic angle spinning (MAS), etc. It can be constructed more easily at room temperature because it does not require thermal insulation, temperature jump, and consideration of the temperature compatibilities of the equipment components and mechanicals. The obtained flexibility allows us to incorporate other useful techniques, e.g., speed-up of MAS (29), as well as reduces the cost. Using photo-excited triplet electrons, new or potential users who have an interest in hyperpolarization can drastically save on the initial and running costs. An extra refrigerator or cryogen is not needed for DNP. The required magnetic field is very low and X-band microwave components are much easier to handle and less expensive than millimeter-wave ones. The most expensive equipment for our experiment is the orange laser. Because pentacene can be excited by a less expensive solid-state green laser with a broad linewidth (23), the cost of hyperpolarization will decrease in the near future.

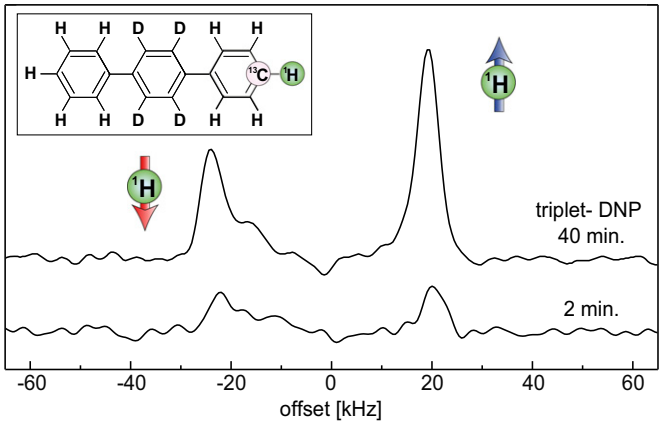

Fig. 3. Asymmetric ^{13}C spectrum. The signals come from naturally abundant ^{13}C spins at the edge of *p*-terphenyl (*Inset*). The spectrum obtained at 11.7 T after 2 min of DNP and that after 40 min are shown.

Until recently, demonstrations of DNP using photo-excited triplet electrons were limited to single crystal and polycrystalline samples (30). In the conventional DNP, a wide variety of samples have been hyperpolarized as a dopant in glassy host materials with polarizing agents (4–8). Recently, in a similar manner, we have also succeeded in polarizing molecules, e.g., 5-fluorouracil, used as antimetabolite, doped in a glassy matrix codoped with pentacene; however, this still required a temperature of 120 K (31). As discussed in ref. 31, to attain a higher polarization at a higher temperature and broaden future applications, we invite contributions from various fields of chemistry and materials science for a suitable glassy host material and polarizing agent with characteristics including high solubility, near unity spin polarization, and harmlessness. High solubility will increase the variety of samples that can be hyperpolarized with DNP. Triplet molecules with electron spin polarization near unity and glassy host materials with longer T_{1n} will enable higher polarizations. For applications to MRI, a study on human body-friendly triplet molecules has the potential to improve the safety, because triplet molecules have no harmful unpaired electrons whereas pentacene itself is harmful for other reasons.

We discuss the scalability of the room temperature hyperpolarization to a larger sample. The required sample volume for in vivo applications is about 40 μL for small animals. ISE efficiency does not depend on the sample volume as long as it is smaller than that of the homogeneous region of the microwave field, which was larger than 40 μL. The required laser power is, in principle, proportional to the number of pentacene molecules in the sample (details are discussed in ref. 32). The irradiated laser with the power of 500 mW is more than enough to excite the present sample doped with 1.3×10^{14} pentacene molecules and can excite up to 1.2×10^{15} pentacene molecules (15). Therefore, the laser power required to excite a 40-μL sample doped with 1.0×10^{16} pentacene molecules is estimated to be 4 W, most of which is converted to heat. This laser-induced heating is much larger than microwave-induced heating. The heating problem can be solved technically, e.g., by increasing the surface area of a sample. In ref. 23, a high-power laser developed for industrial use was already used in photo-excited triplet DNP and the authors achieved hyperpolarization of an 80-μL sample at 77 K.

DNP using photo-excited triplet electrons can be also applied in fundamental physics experiments. Bulk nuclear hyperpolarization in such low magnetic fields is desirable for scattering experiments with unstable nuclei, neutrons, and elementary particles (3, 33). The low entropic state of a bulk nuclear spin ensemble can be used for quantum information processing experiments: quantum sensing toward single nuclear spin detection (34–36), quantum computing (37), and studies on magnetic phase transition, which is presently a hot topic in quantum simulation (38, 39) and was previously investigated by Abragam et al. at sub-Kelvin temperatures (1).

In conclusion, by using electron spins in photo-excited triplet states, we can acquire a higher DNP enhancement factor than the conventional limit, 660, using electron spins in thermal equilibrium, while maintaining a bulk sample at room temperature. By deuteration of the polarizing agent and regioselective deuteration of the host, we have achieved the ^{1}H spin polarization of 34%. Such a high polarization was proved by the asymmetric spectrum. The room temperature hyperpolarization technique can be applied in areas of chemistry, materials science, biology, and medical science as well as fundamental physics.

Materials and Methods

We purchased *p*-terphenyl and pentacene from Sigma-Aldrich. Deuterated pentacene was given to us by Kazuyuki Takeda, Kyoto University. He purchased it from Icon Isotopes. *p*-Terphenyl-2′,3′,5′,6′-d_4 was synthesized in the way shown in *SI Text*. *p*-Terphenyl and *p*-terphenyl-2′,3′,5′,6′-d_4 were purified by zone refining. Pentacene and deuterated pentacene were used without further purification. Single crystals of *p*-terphenyl (-2′,3′,5′,6′-d_4) doped with ∼0.05 mol% (deuterated) pentacene were grown by the Bridgman method. They were cut into pieces with a size of ∼0.7 × 0.7 × 1 mm^3 and mounted in a cylindrical cavity (TE_{011} mode tuned at 12.05 GHz) so that the long axis of the pentacene molecules was parallel to the static magnetic field (34, 40, 41). The total number of the spins in the sample is $>10^{19}$ and the density is $>2\times10^{22}$ spins per cubic centimeter. Pentacene was excited with a flashlamp-pumped dye laser (Cynosure; LFDL-3). The pulse width and energy were 1 μs and 10 mJ. A microwave pulse with the frequency of 12.05 GHz was applied with the cavity. The width and strength of microwave pulse and the width of field sweep are summarized in *SI Text*. ^{1}H NMR at 0.40 T was detected by tip pulse with the rotation angle of 3° at 17.2 MHz. We carried out DNP at the repetition rate of 50 Hz. The NMR experiments and timing control of the DNP, which are shown together with the details of the experimental setup and NMR spectra in *SI Text*, were programmed with an OPENCORE NMR spectrometer (42, 43). The enhancement factor was calculated by comparing the integrated intensities of the ^{1}H NMR signal S_{etha} of ethanol (40.7 mg) in thermal equilibrium in 0.40 T at 300 K and the hyperpolarized signal S_{DNP}. The polarization was calculated by

$$P=\frac{N_{etha}}{N_{DNP}}\frac{S_{DNP}}{S_{etha}}\tanh\left(\frac{\hbar\gamma B}{2kT}\right), \quad [2]$$

where N_{etha} is the number of the ^{1}H spins in the sample of ethanol and N_{DNP} is that in the hyperpolarized sample. The ^{1}H spin polarization was also determined from the ratio of the asymmetric spectrum of ^{13}C spin, for which the field-cycling instrumentation and the NMR sequence with cross polarization are shown in *SI Text*.

ACKNOWLEDGMENTS. We thank Kazuyuki Takeda for fruitful discussions and supplying deuterated pentacene. This work was supported by The Ministry of Education, Culture, Sports, Science and Technology (MEXT) Grant-in-Aid for Scientific Research on Innovative Areas 21102004 and the Funding Program for World-Leading Innovative R&D on Science and Technology. K.T. was also supported by the Global-Center Of Excellence (COE) Program of Osaka University.

1. Abragam A, Goldman M (1982) *Nuclear Magnetism: Order and Disorder* (Clarendon, Oxford).
2. Crabb DG, Meyer W (1997) Solid polarized targets for nuclear and particle physics experiments. *Annu Rev Nucl Part Sci* 47:67–109.
3. Obertelli A, Uesaka T (2011) Hydrogen targets for exotic-nuclei studies developed over the past 10 years. *Eur Phys J A* 47(9):105.
4. Lesage A, et al. (2010) Surface enhanced NMR spectroscopy by dynamic nuclear polarization. *J Am Chem Soc* 132(44):15459–15461.
5. Ardenkjaer-Larsen JH, et al. (2003) Increase in signal-to-noise ratio of > 10,000 times in liquid-state NMR. *Proc Natl Acad Sci USA* 100(18):10158–10163.
6. Maly T, et al. (2008) Dynamic nuclear polarization at high magnetic fields. *J Chem Phys* 128(5):052211.
7. Bajaj VS, Mak-Jurkauskas ML, Belenky M, Herzfeld J, Griffin RG (2009) Functional and shunt states of bacteriorhodopsin resolved by 250 GHz dynamic nuclear polarization-enhanced solid-state NMR. *Proc Natl Acad Sci USA* 106(23):9244–9249.
8. Gallagher FA, et al. (2008) Magnetic resonance imaging of pH in vivo using hyperpolarized 13C-labelled bicarbonate. *Nature* 453(7197):940–943.
9. Overhauser AW (1953) Polarization of nuclei in metals. *Phys Rev* 92:411–415.
10. Carver TR, Slichter CP (1953) Polarization of nuclear spins in metals. *Phys Rev* 92: 212–213.
11. Meier F, Zakharchenya BP (1984) Optical Orientation, *Modern Problems in Condensed Matter Sciences* (North Holland, Amsterdam), Vol 8.
12. Horsewill AJ (2000) Quantum tunneling aspects of methyl group rotation studied by NMR. *Prog Nucl Magn Reson Spectrosc* 35(4):359–389.
13. Henstra A, Lin T-S, Schmidt J, Wenckebach WTh (1990) High dynamic nuclear-polarization at room-temperature. *Chem Phys Lett* 165(1):6–10.
14. Stehlik D, Vieth HM (1992) *Pulsed Magnetic Resonance NMR, ESR and Optics* (Oxford Univ Press, New York), pp 446–477.
15. Takeda K, Takegoshi K, Terao T (2004) Dynamic nuclear polarization by electron spins in the photoexcited triplet state: 1. Attainment of proton polarization of 0.7 at 105 K in naphthalene. *J Phys Soc Jpn* 73:2313–2318.
16. Takeda K (2009) *Triplet State Dynamic Nuclear Polarization* (VDM, Saarbrücken, Germany).
17. Sloop DJ, Yu H-L, Lin T-S, Weissman SI (1981) Electron spin echoes of a photoexcited triplet: Pentacene in p-terphenyl crystals. *J Chem Phys* 75:3746–3757.
18. Ong JL, Sloop DJ, Lin TS (1995) Deuteration effect on the spin dynamics of the photoexcited triplet-state of pentacene in p-terphenyl crystals. *Chem Phys Lett* 241: 540–546.
19. Iinuma M, et al. (2005) Proton polarization with p-terphenyl crystal by integrated solid effect on photoexcited triplet state. *J Magn Reson* 175(2):235–241.
20. Kohda K, Nakamura N, Chihara H (1982) Proton magnetic relaxation study of phase transition in crystalline p-terphenyl. *J Phys Soc Jpn* 51:3936–3941.
21. Kagawa A, Murokawa Y, Takeda K, Kitagawa M (2009) Optimization of 1H spin density for dynamic nuclear polarization using photo-excited triplet electron spins. *J Magn Reson* 197(1):9–13.
22. van den Heuvel DJ, Schmidt J, Wenckebach WTh (1994) Polarizing proton spins by electron-spin locking of photo-excited triplet state molecules. *Chem Phys* 187: 365–372.
23. Eichhorn TR, Haag M, van den Brandt B, Hautle P, Wenckebach WTh (2013) High proton spin polarization with DNP using the triplet state of pentacene-d_{14}. *Chem Phys Lett* 555:296–299.
24. Eichhorn TR, van den Brandt B, Hautle P, Henstra A, Wenckebach W (2013) Dynamic nuclear polarisation via the integrated solid effect II: experiments on naphthalene-h8 doped with pentacene-d14. *Mol Phys*, 10.1080/00268976.2013.863405.
25. Waugh JS, Gonen O, Kuhns P (1987) Fourier transform NMR at low temperatures. *J Chem Phys* 86:3816–3818.
26. Morley GW, et al. (2007) Efficient dynamic nuclear polarization at high magnetic fields. *Phys Rev Lett* 98(22):220501.
27. Gitti R, et al. (1988) Solid/liquid intermolecular transfer of dynamic nuclear polarization. Enhanced flowing fluid proton NMR signals via immobilized spin labels. *J Am Chem Soc* 110:2294–2296.
28. Kagawa A, Negoro M, Takeda K, Kitagawa M (2009) Magnetic-field cycling instrumentation for dynamic nuclear polarization-nuclear magnetic resonance using photoexcited triplets. *Rev Sci Instrum* 80(4):044705.
29. Nishiyama Y, et al. (2011) Very fast magic angle spinning (1)H-(14)N 2D solid-state NMR: Sub-micro-liter sample data collection in a few minutes. *J Magn Reson* 208(1): 44–48.
30. Takeda K, Takegoshi K, Terao T (2001) Dynamic nuclear polarization by photoexcited-triplet electron spins in polycrystalline samples. *Chem Phys Lett* 345(1-2):166–170.
31. Tateishi K, Negoro M, Kagawa A, Kitagawa M (2013) Dynamic nuclear polarization with photoexcited triplet electrons in a glassy matrix. *Angew Chem Int Ed Engl* 52(50): 13307–13310.
32. Takeda K, Takegoshi K, Terao T (2002) Zero-field electron spin resonance and theoretical studies of light penetration into single crystal and polycrystalline material doped with molecules photoexcitable to the triplet state via intersystem crossing. *J Chem Phys* 117:4940–4946.
33. Haag M, van den Brandt B, Eichhorn TR, Hautle P, Wenckebach WTh (2012) Spin filtering neutrons with a proton target dynamically polarized using photo-excited triplet states. *Nucl Instrum Methods Phys Res A* 678:91–97.
34. Negoro M, Tateishi K, Kagawa A, Kitagawa M (2011) Scalable spin amplification with a gain over a hundred. *Phys Rev Lett* 107(5):050503.
35. Mamin HJ, et al. (2013) Nanoscale nuclear magnetic resonance with a nitrogen-vacancy spin sensor. *Science* 339(6119):557–560.
36. Staudacher T, et al. (2013) Nuclear magnetic resonance spectroscopy on a (5-nanometer)^3 sample volume. *Science* 339(6119):561–563.
37. Cory DG, et al. (2000) NMR based quantum information processing: Achievements and prospects. *Fortschr Phys* 48:875–907.
38. Roumpos G, Master CP, Yamamoto Y (2007) Quantum simulation of spin ordering with nuclear spins in a solid-state lattice. *Phys Rev B* 75:094415.
39. Buluta I, Nori F (2009) Quantum simulators. *Science* 326(5949):108–111.
40. Rietveld HM, Maslen EN, Clews CJB (1970) An X-ray and neutron diffraction refinement of the structure of p-terphenyl. *Acta Crystallogr* 26:693–706.
41. van Strien AJ, Schmidt J (1980) An EPR study of the triplet state of pentacene by electron spin-echo techniques and laser flash excitation. *Chem Phys Lett* 70:513–517.
42. Takeda K (2007) A highly integrated FPGA-based nuclear magnetic resonance spectrometer. *Rev Sci Instrum* 78(3):033103.
43. Takeda K (2008) OPENCORE NMR: Open-source core modules for implementing an integrated FPGA-based NMR spectrometer. *J Magn Reson* 192(2):218–229.